Morphology-Controlled Synthesis of Monodisperse ZnO Troughs at the Air−Water Interface under Mild Conditions

Jiang Tang,[†,‡] Xiaoqiang Cui,[†] Yang Liu,[†,‡] and Xiurong Yang*[,†,‡]

State Key Laboratory of Electroanalytical Chemistry, Changchun Institute of Applied Chemistry, Chinese Academy of Sciences, Changchun, Jilin 130022, China and Graduate School of the Chinese Academy of Science, Beijing 100039, China

Received: August 2, 2005; In Final Form: September 20, 2005

In this work, an interfacial synthetic strategy to produce ZnO troughs at the air−water interface under mild conditions was demonstrated. The as-prepared ZnO trough was monodisperse, single crystalline, and pure. By manipulation of the magnet stirring time, the fabricated ZnO can be manipulated as an independent or intertwined trough. Various preparative parameters, such as initial reactants and their concentrations, had been examined, and the results revealed that troughlike ZnO could be only obtained by adopting zinc acetate and hexamethylenetetramine as precursors at concentrations larger than 0.01 M. The as-obtained ZnO, within the dimension of several micrometers, showed a trough-related photoluminescence emission at 356 nm. Moreover, the evolution process of a ZnO trough after reaction for 5, 30, 60, and 90 min was viewed by X-ray diffraction and field emission scanning electron microscopy characterization, and a possible mechanism was also proposed and discussed, which might help us to further our understanding toward the reaction mechanism at the air−water interface.

Introduction

Semiconductor nanomaterials have attracted much attention. Their interesting electronic and optical properties inherently associated with quantum confinement effect make them a potential representative for nanoscale device construction in the future. Among these materials, the VI−II n-type semiconductor material ZnO, with a wide and direct band gap of 3.37 eV and a large exciton binding energy (60 meV), which is much greater than thermal energy at room temperature, is considered to be a promising candidate for applications in blue−UV light emission and room-temperature UV lasing.[1−4] Furthermore, ZnO has promising applications in catalysis,[5] gas sensors,[6] electrical devices,[7,8] transparent thin films,[9] solar cells,[10] and surface acoustic wave devices.[11]

Synthesis of size- and shape-controlled ZnO nanostructures is very important in controlling their physical, chemical, and optical properties,[5,12] which is crucial for their potential use. Various morphologies of ZnO, such as nanowire,[13,14] nanobridges, and nanonails,[15] nanohelixes and nanosprings,[16] and so on have been synthesized through vapor-based methods. Moreover, nanoneedle,[17] flowerlike,[18,19] hexagonal disks and rings,[20] dandlieons,[21] and flowerlike cupped microrod bundles[22] of ZnO have also been conveniently synthesized in aqueous solution recently. The as-synthesized ZnO shows morphology-dependent properties, which triggers and accelerates the intense research on the synthesis of various morphological ZnO through many approaches.

Interestingly, there are plenty of papers concerned with the exploitation of producing ZnO in solution, while interface synthesis seemed to be ignored. To our knowledge, there are no reports concerned with the synthesis of ZnO at an interface, where a different environment would be provided and novel morphology and properties could be expected. To test our supposition, we selected and modified a well-developed method, which was proposed by Vayssieres[23,24] and O'Brien[25,26] and showed great success in synthesizing highly oriented ZnO films, to synthesize ZnO at the air−water interface. As expected, the as-prepared troughlike ZnO, a new member to the ZnO family, was uniform and of high purity. In addition, photoluminescence examination showed a novel trough-related UV emission centered at 356 nm, which was rare for a several micrometer ZnO trough. Moreover, control experiments clearly indicated that troughlike ZnO could only be produced at the air−water interface, with zinc acetate and hexamethylenetetramine as precursors at concentrations greater than 0.01 M. Finally, evolution of the troughlike ZnO was investigated by X-ray diffraction (XRD) and field emission scanning electron microscopy (FE-SEM) characterization, and a two-step grown mechanism was revealed: forming of ZnO twinning universally and then some evolving into troughlike ZnO at the air−water interface.

Experimental Section

Anhydrous zinc acetate ($Zn(OOCCH_3)_2$), hexamethylenetetramine ($(CH_2)_6N_4$, HMT), zinc chloride ($ZnCl_2$), and hydrazine hydrate ($N_2H_4 \cdot 2H_2O$, v/v = 1:1) were analytical grade, purchased from Alfa Aesar, and used as received without further purification. Major experiments carried out in this work are summarized in Table 1. In a typical synthesis, 20 mL of aqueous solution of zinc acetate and 20 mL of hexamethylenetetramine aqueous solution of equal concentration were mixed together and kept under mild magnetic stirring for a given time (10 or 30 min). The solution was slightly turbid, which indicated nucleation at room temperature. Then the solution was transferred to a 250 mL uncovered beaker (8 cm in diameter, 50.24 cm^2) and heated at 90 °C for 1 h or 1.5 h. The beaker was kept undisturbed and no air flow was exerted over the surface.

* Corresponding author. Tel: +86-0431-5689278. E-mail: xryang@ciac.jl.cn.

† State Key Laboratory of Electroanalytical Chemistry, Changchun Institute of Applied Chemistry, Chinese Academy of Sciences.

‡ Graduate School of Chinese Academy of Science.

10.1021/jp054286b CCC: $30.25
Published on Web 10/20/2005

TABLE 1: Sample Numbers, Initial Chemicals, Reaction Conditions, and Obtained Morphologies in the Synthesis

sample no.	reactants	concn[a] (M)	magnet stirring time (min)	heating time (min)	morphology
A	$Zn(Ac)_2$ and HMT	0.1	10	60	independent trough
B	$Zn(Ac)_2$ and HMT	0.1	30	60	intertwined trough
C	$Zn(Ac)_2$ and HMT	0.01	10	60	solid twinning rod
D	$Zn(Ac)_2$ and HMT	0.05	10	60	independent trough
E	$Zn(Cl)_2$ and HMT	0.1	10	90	hexagonal flake
F	$Zn(Ac)_2$ and hydrazine[a]	0.1	10	90	flower

[a] The concentration and the aqueous solution volume of zinc salt and the amine were equal. [b] 20 mL of 0.1 M $Zn(Ac)_2$ and 4 mL of hydrate hydrazine (v/v = 1:1).

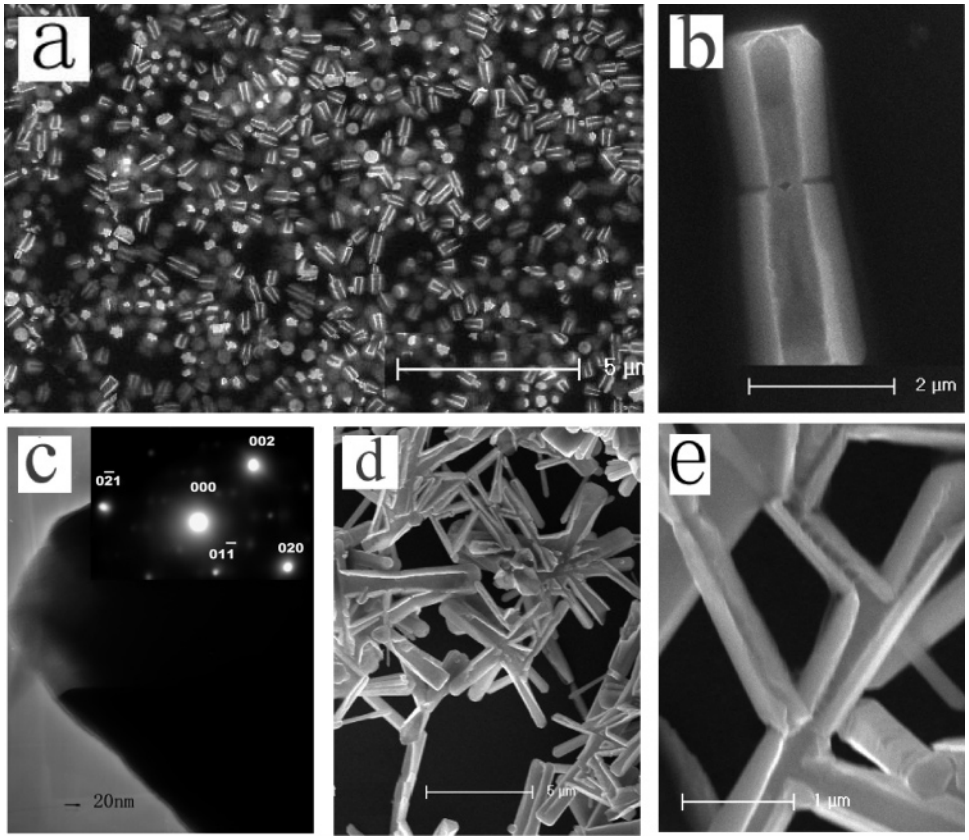

Figure 1. FE-SEM and TEM images of the as-prepared ZnO products: (a) troughlike ZnO gained at the air−water interface in sample A; (b) high-magnification image of a single ZnO trough; (c) TEM image of a typical trough and its SAED pattern recorded along the (100) zone axis (inset); (d) ZnO trough obtained at the air−water interface of sample B; (e) its high-magnification image.

The resulted solution became clear, and a film of white product covered the air−water interface with sediments in the bottom. Then the product was collected, rinsed three times with deionized water and anhydrous ethanol, and dried in the open air for further characterization.

X-ray power diffraction (XRD) analysis was conducted on a Rigaku D/max-2500 X-ray diffractometer with graphite monochromated Cu Kα radiation ($\lambda = 1.5418$ Å). Room-temperature fluorescence measurement was carried out on a Pekin-Elmer LS 50B spectrometer by exciting the sample with a He−Cd laser at 315 nm. Thermogravimetric (TG) analysis was carried out with a Netszch STA 409C in a N_2 atmosphere at a temperature range from 25 to 800 °C, with a heating rate of 5 °C·min^{-1}. The sample morphology was examined by field-emission scanning electron microscopy (FE-SEM) and transmission electron microscopy (TEM). It should be emphasized that except for only one sample (the 5 min sample in the evolution characterization series) that adopted the posttreatment mentioned above, all other samples for the FE-SEM and TEM characterization were prepared by directly transferring the suspended products at the air−water interface, without any treatment, to the ITO glass slide and standard carbon-coated Formvar film on copper grid, respectively. FE-SEM analysis and X-ray energy dispersion spectrum (EDS) were conducted on a Philips XL-30 field-emission scanning electron microscope operated at 15 kV, while TEM and selected area electron diffraction (SAED) were performed on a JEOL-JEM-2010 (JEOL, Japan) electron microscope operating at 200 kV.

Results and Discussion

Structure and Morphology. The morphology of the obtained ZnO was characterized by FE-SEM and TEM and typical images are shown in Figure 1. With a shorter stirring time (sample A), uniform ZnO twinning rods, connected together by two hexagonal prisms accompanied with troughs in, were abundantly obtained at the air−water interface (Figure 1a). All the troughs were independent, separate, and showed small size distribution in length and width. A high-resolution image of Figure 1b revealed that the trough connected at the grain boundary and the inner plane was coarse. A TEM image (Figure 1c) of a single ZnO trough confirmed the observation of troughs in the twinning. The inset is a SAED pattern recorded along

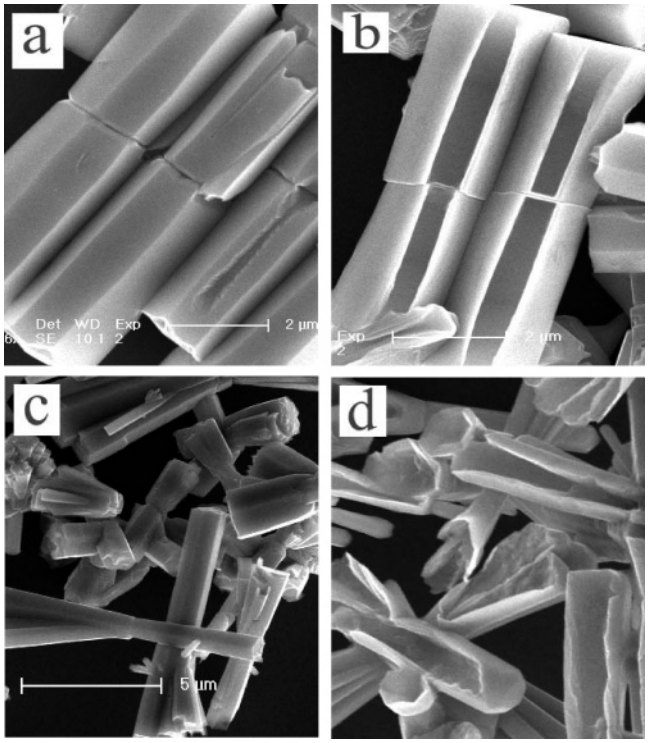

Figure 2. Morphology comparison of ZnO products: (a) in solution of sample A; (b) at the air−water interface of sample A; (c) in solution of sample B; (d) at the air−water interface of sample B.

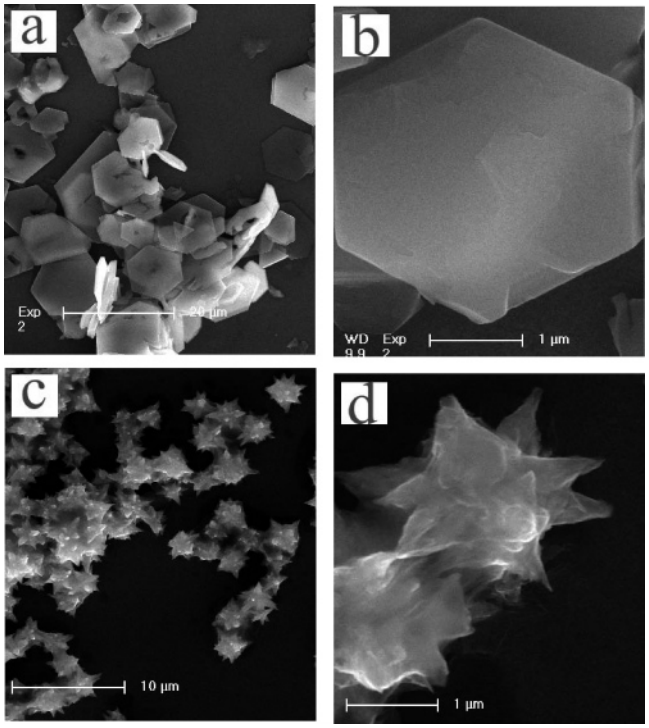

Figure 3. FE-SEM images of the ZnO samples with different reactants: (a) low-resolution image and (b) a single hexagonal ZnO flake of sample E ($Zn(Cl)_2$ and HMT); (c) low-resolution image; (d) a single flowerlike ZnO of sample F ($Zn(Ac)_2$ and hydrazine).

the (100) zone axis of a single ZnO trough, and it clearly indicated that the ZnO trough was single crystalline and grew along the (0001) direction. It should be pointed out that in the FE-SEM observations, all ZnO twinning had troughs in. The one observation where no troughs were observed was because the surface on which the troughs were is opposite or perpendicular to the observer. Noting that the product was not washed and purified, its high purity merits such a synthetic strategy. The high purity of the product was derived from the "self-selective effect", which will be delivered in detail in the later part of this paper.

For a longer stirring time (sample B), the morphology of the as-prepared ZnO was different and is shown in panels d and e of Figure 1. ZnO twinning character, as well as the well discernible crystal faces, is no longer apparent. The troughs, about 5 μm long and several hundred nanometers wide, interlaced with each other to form a net. In sample A, troughs seemed to be "dug out" in one side face of the twinning, while in sample B, they seemed to be formed through curled ZnO ribbon. High-magnification SEM observation further illustrated that most troughs branched and connected with each other, whereas single troughs also existed.

Comparison of the morphology of ZnO obtained in solution and at the air−water interface had also been carried out by FE-SEM observation, and the results are shown in Figure 2. In the sediments of sample A, a large number of solid ZnO twinning rods, well crystalline yet without troughs, were abundantly obtained. While for the ZnO products suspended at the air−water, these products were also twinning and had the same dimension as the ZnO precipitates. Nevertheless, all of them coupled with regular troughs on the same side, as clearly indicated in Figure 2b. With sample B, the results were the same. The morphology of ZnO obtained at the air−water interface was similar to the ones harvested in solution, and the only difference was that they possessed troughs. These results justified the conclusion that ZnO troughs only could be produced at the air−water interface. Since in this system, the morphology of ZnO produced at the interface resembled the ZnO obtained in solution, we can conveniently tune the morphology of ZnO trough at the air−water interface by manipulating the reaction conditions and parameters.

Effects of Reaction Conditions. To examine the influence of the reactants, we replaced one reactant and kept the other experimental variables unchanged. The morphologies of two control experimental products collected at the air−water interface of sample E (20 mL of 0.1 M zinc chloride reacted with 20 mL of 0.1 M hexamethylenetetramine) and sample F (20 mL of 0.1 M zinc acetate reacted with 4 mL of hydrate hydrazine) are shown in Figure 3. In sample E, hexagonal flakes, several micrometers in diameter and tens of nanometers in thickness, had been abundantly obtained, as illustrated in Figure 3a. The as-obtained ZnO flakes were perfect crystals but of poor monodispersivity and integrity. Moreover, some of the flakes had a hole at the middle, which resembled the observation by Wang et al.[20] In sample F, we had produced monodisperse flowerlike ZnO, which is similar to the reports of many other groups.[18,19,25] Notably, no troughlike ZnO was observed in either sample.

In another set of experiments, we simply changed the concentration of the $Zn(OOCH_3)_2$ and HMT while keeping their ratio constant to investigate effects of the reactant concentration, and the products collected at the air−water interface of sample C (0.01 M) and sample D (0.05 M) are present in Figure 4. In sample C, ZnO nanorods which were partly hollowed in the end, instead of troughlike ZnO, had been successfully achieved, as illustrated in panels a and b of Figure 4. Once the concentration was increased to 0.05 M, monodisperse, independent troughlike ZnO was successfully obtained and the troughs in the side face of hexagonal ZnO prisms correspond to the dark parts in Figure 4c. The typical length, width of trough, and thickness of the wall is about 6.9 μm, 640 nm and 80 nm,

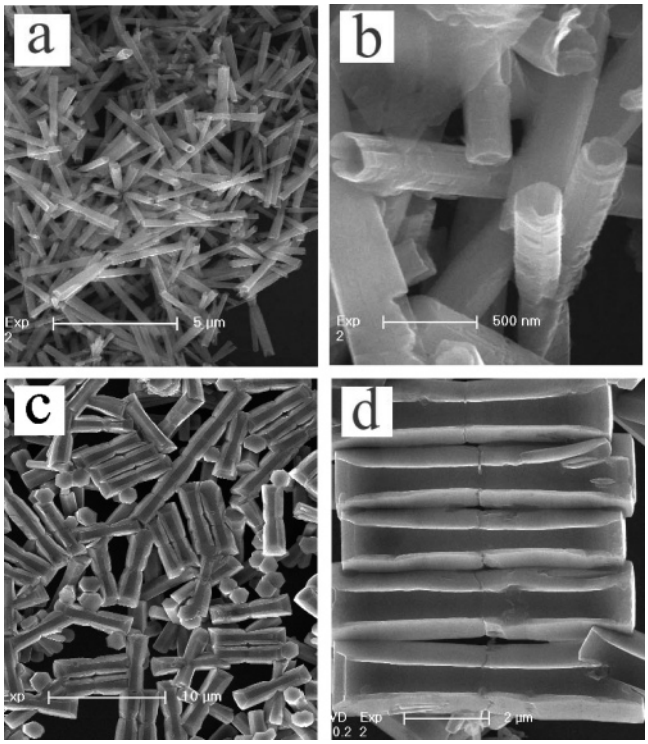

Figure 4. The morphologies of the as-synthesized ZnO adopted $Zn(Ac)_2$ and HMT as the reactants with different concentrations: (a) low-resolution and (b) high-resolution images of ZnO products in sample C (0.01 M); (c) low-resolution and (d) high-resolution images of ZnO products in sample D (0.05 M).

respectively, examined by using the ruler in the FE-SEM program. On the basis of the results mentioned above, we could conclude that there are two prerequisites to synthesize troughlike ZnO at the air−water interface: use zinc acetate and hexamethylenetetramine as precursors and maintain their concentrations higher than a critical value.

Morphology Evolution. To understand the growing mechanism, the suspended products (in sample A) after reacting for 5, 30, 60, and 90 min were collected for FE-SEM and XRD characterization. Figure 5 shows the evolution of the ZnO nanostructures as a function of reaction time. FE-SEM observation of the sample which aged at 90 °C for only 5 min revealed that white particles, about 400 nm in diameter, were randomly scattered in the "cloud", as illustrated in Figure 5a. Select point EDS analysis of the white particles showed an atomic ratio of Zn:O ≈ 1:1 and the content of C and N elements were negligible; hence we could conclude that the white substance was ZnO. In addition to this, EDS and TG examination were also conducted to analyze the opaque "cloud". Full screen EDS analysis gave an atomic ratio of Zn:O:C = 26.3:51.3:22.4 and TG examination of the sample showed a weigh loss of 4.6% at 97.6 °C and a weight loss of 30.0% up to 540 °C, which was related to the procedure of dehydration and acetate molecule removal, respectively. The "cloud" intermediate can be expressed by the formula $ZnO{\cdot}0.76Zn(OOCCH_3)_2{\cdot}0.46H_2O$, yet further analysis should be done in future work. Since the intermediate $ZnO{\cdot}0.76Zn(OOCCH_3)_2{\cdot}0.46H_2O$ was unstable and suspended on the surface, it played a dual role in ZnO trough forming: gradually decomposing to provide materials for ZnO growth and loading ZnO particles at the air−water surface. These ZnO particles interspersed in the cloud and served as seeds for further growth. Moreover, we had also centrifugated and rinsed the sample to discard the intermediate for a better FE-SEM characterization, and the result is shown in Figure 5b.

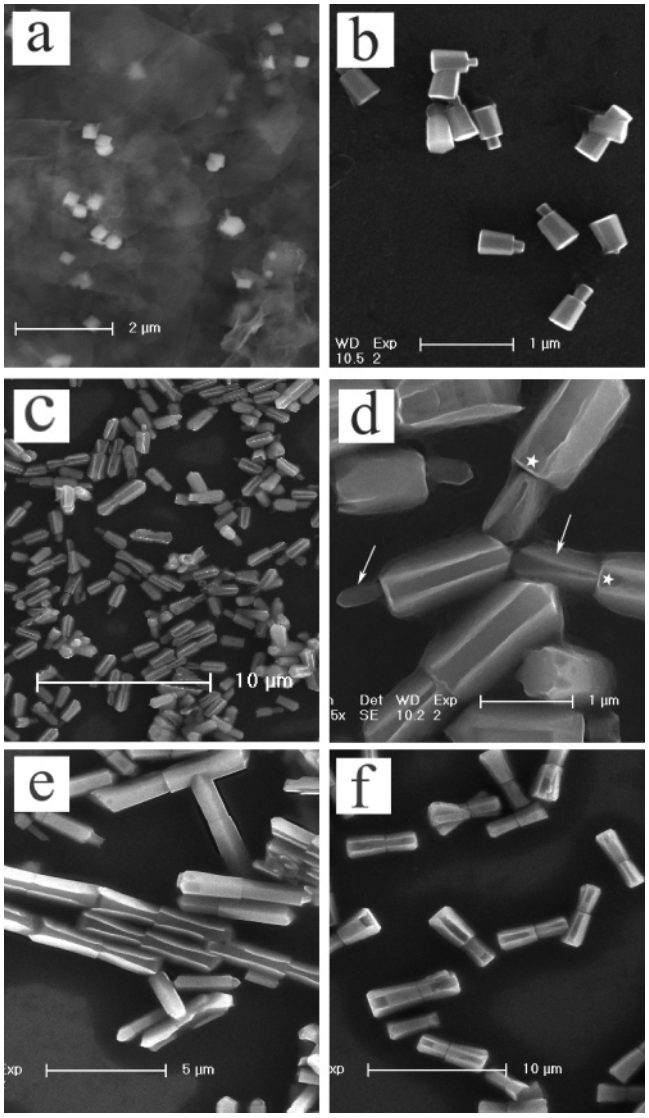

Figure 5. FE-SEM images of the ZnO products collected at the air−water interface in sample A at different times: (a) 5 min without any treatment; (b) 5 min with centrifugation and rinse; (c) and (d) 30 min; (e) 60 min; (f) 90 min.

In contrast with Figure 5a, the "cloud" no longer exists and the ZnO particles turned out to be well-crystalline ZnO hexagonal cones attached by a "bud". The cone was about 300 nm in width and 500 nm in length, while the "bud" was 50 nm wide and 60 nm long. To our knowledge, this is the first report of direct observation of the development of ZnO twinning. In a word, the overall results showed no troughlike ZnO formed at this stage.

However, as the reaction time was extended to 30 min, ZnO twinning, each with two troughs embedded, appeared and was abundantly seen (Figure 5c). The troughs were about 2 μm long on average, and the ZnO twinning was asymmetrical, since one subunit was larger than the other. The troughs developed well and were rectangular in the larger subunit of twinning, while in the smaller counterpart troughs weere not well developed and remained narrower in the grain boundary side. In some cases, no trough was observed in the smaller subunit, as the arrows indicated in Figure 5d. It is apparent that the larger and the smaller subunit of the twinning derived from the cone and the "bud", respectively. Moreover, there were two well-developed ZnO $(000\bar{1})$ planes at the grain boundary, as indicated by the stars, which provide some clues for the understanding

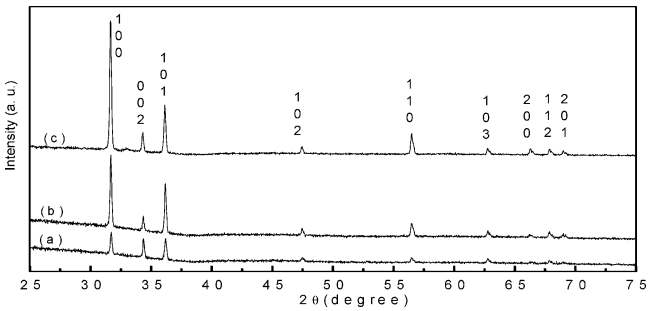

Figure 6. XRD patterns of the ZnO harvested at the air−water interface in sample A at different times: (a) 5 min; (b) 30 min; (c) 60 min.

of the growth mechanism. Besides, there were still some "clouds" adhering to the surface of the troughlike ZnO, which revealed that $ZnO{\cdot}0.76Zn(OOCCH_3)_2{\cdot}0.46H_2O$ had not completely decomposed after reacting for 30 min. When the reaction proceeded to 60 min, the trough grew larger and longer and showed better crystal perfection. The smaller subunit of the twinning had evolved to be equivalent with the bigger one, and the twinning was no longer asymmetrical. Both subunits possessed a full-developed rectangular trough and connected with each other at the grain boundary. No "cloud" was detectable in this stage. Thus, it seemed 60 min was long enough to produce well-developed troughlike ZnO and completely decompose the intermediate. On further prolonging the reaction to 90 min, the ZnO trough was as large as it was at 60 min, about 5 μm in length, which indicated that the twinning growth had stopped. Nevertheless, in this stage some troughs were partly covered by slices, though the troughs remained discernible, as shown in Figure 5f.

XRD measurement of the ZnO suspended products sampled at varied time also had been carried out and is shown in Figure 6. It can be seen that the diffraction peaks of each sample display a wurtzite structure and are in good agreement with the JCPDS file of ZnO (JCPDS 36-1451; wurtzite-type, space group $P6_3mc$). No impurities were observed in these patterns. Moreover, the sharp diffraction peaks indicated that the samples were highly crystalline, which corresponds well to the FE-SEM and SAED observations.

Growth Mechanism. It is well-known that elongated hexagonal ZnO crystal grows along the *c*-axis and has both polar and nonpolar surfaces. The former is the zinc-terminated (0001) face and the oxygen-terminated $(000\bar{1})$ face while the latter includes the $(10\bar{1}0)$ and $(11\bar{2}0)$ face. The nonpolar crystal faces are more energy favorable and hence more stable than those polar ones. Moreover, in our synthetic systems HMT serves as a pH buffer to release OH^-, and OH^- subsequently reacts with Zn^{2+} to form $Zn(OH)_4^{2-}$. In addition, ZnO has the propensity to twin,[25−28] and under our experimental conditions it grows via orientated aggregation of nanoparticles and subsequent development of single crystalline material by dissolution−reprecipitation.[26] Thus, we believed in our system two different fashions were adopted and resulted in distinct morphologies of ZnO. In solution, growth units could diffuse into ZnO nanoparticles from all directions, stacked in each crystal face, and thus solid ZnO twinning was obtained. Contrarily, $ZnO{\cdot}0.76Zn(OOCCH_3)_2{\cdot}0.46H_2O$—the "cloud"—was first formed and suspended at the air−water interface. The intermediate not only decomposed into ZnO nanoparticles as the reaction proceeded but also loaded such ZnO particles serving as seed for the further growth. At this stage, the intermediate was thick enough to encompass the ZnO nanoparticles, so ZnO particles could receive growth units decomposed by the intermediate in all directions and solid ZnO cones were obtained. This process might correspond to the first 5 min. However, as the reaction proceeded, intermediate was gradully consumed and the film became thinner and thinner. Growth units could diffuse only onto ZnO particles' planes which contacted with water or embedded in the film, so these planes grew freely. No growth occurred on the ZnO crystal face, which was toward the air side. As a result, the ZnO nanostructures became hollow and thus trough was formed. The trough prolonged correspondingly as the growth of ZnO along the *c*-axis and deepened following the development of the side faces. This hypothesis is justified by our observation: The smaller subunit of the ZnO twinning was solid in Figure 5d. It was so small that it could immerse into water or the intermediate film even when the intermediate film was too thin for the larger subunit to embed in. The observation of two $(000\bar{1})$ planes at the grain boundary, as indicated by the star symbols in Figure 5d and confirmed by our observations in other samples. Because of the crack at the grain boundary, growth units could diffuse to the boundary from the solution and well-developed polar $(000\bar{1})$ planes formed. It should be pointed out that the intermediate thin film might play a key role in the trough forming. Failure to produce such a proper film (samples E and F) or the film not being thick enough to load or embed ZnO particles (sample C), no ZnO trough could be obtained in these samples.

As the trough-like ZnO formed, the ZnO trough began to float on the air−water interface like a boat, and the growth of the trough was further favored—growth occurred only at the bottom and the side planes of the "boat"—and the trough further became much deeper and larger. At the same time, the dissolution−reprecipitation process flattened the immersed surface and this process was impossible for the inner surface of the trough, so these inner planes were coarse as initially stacked. When reacted for 90 min, the intermediate film was completely exhausted and the ZnO trough was suspended at the air−water surface due to buoyancy and surface tension. The

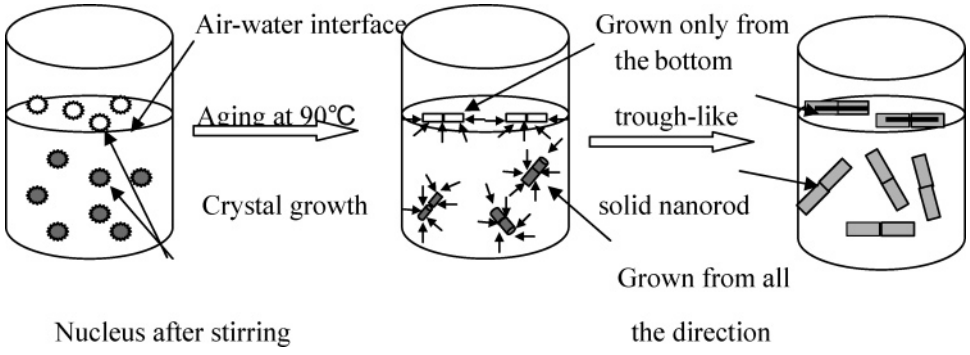

Figure 7. Schematic diagram illustration of ZnO nanostructure evolution at the air−water interface and in the bulk solution.

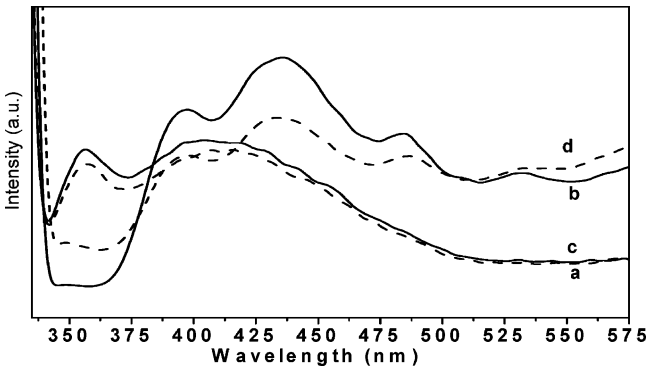

Figure 8. Comparison of photoluminescence spectra ($\lambda_{ex} = 315$ nm) of the obtained ZnO: (a) independent ZnO trough at the air−water interface and (b) solid ZnO twinning in the solution of sample A (solid line); (c) intertwined ZnO trough at the air−water interface; (d) solid ZnO rods in the solution of sample B (dash line).

plane toward air side might be immersed or wetted by solution, leading to the formation of partly covered slices (Figure 5f). It should be noticed that at this stage all the solid twinning would sink into the solution, leaving only troughs suspend at the air−water interface—we call it a "self-selective effect", which resulted in the high purity of the troughlike ZnO at the air−water interface. The growth mechanism was also schematically illustrated in Figure 7.

Photoluminescence. To exploit its optical property, room-temperature photoluminescence of ZnO was measured and is shown in Figure 8. It indicated that solid ZnO without troughs, obtained in the solution of sample A and sample B, showed three photoluminescence peaks at 396, 435, and 484 nm. The UV emission should be attributed to near band-edge emission of the wide band gap of ZnO, and the green photoluminescence was assigned to recombination of photoexcited electrons (e^-) with deeply trapped holes in the singly ionized oxygen vacancy ($V^{\bullet}_O$).[28,29] The blue emission, though very rare but has been also observed by others,[22] was inherent in this preparation method. It may be caused by the surface defects or absorbents, the reason remains not yet clear.[30] Very interestingly, as for the troughlike ZnO produced at the air−water interface in sample A and sample B, a narrow UV emission centered at 356 nm and a broad blue emission were observed. The broad blue peak should be assigned as the overlay of the three emissions, and it was also observed in the solid ZnO without troughs. The UV emission at 356 nm was strong and narrow. On the basis of the facts that the sediments in sample A did not show the 356 nm peak, and the troughlike ZnO in sample B also possessed the 356 nm peak, we can rule out the possibility that it is due to the twinning. Hence, we can assign the blue shift of the band emission, from 3.37 eV in bulk ZnO to 3.48 eV, which indicated clearly the confinement effect, to the special trough morphology. Furthermore, O'Brien et al. reported that the surface of ZnO twinning is composed of 5 nm ZnO nanoparticles and subsequently developed into a single crystalline by dissolution−reprecipitation.[26] Since the inner part of the ZnO could never experience such a dissolution−reprecipitation process, we believed that such 5 nm ZnO nanoparticles in the ZnO trough might be responsible for the 356 nm emission. However, the mechanism is still not yet clear and investigation is under way.

Conclusion

In conclusion, we have developed a strategy to synthesize novel troughlike ZnO at the air−water interface. This method is template-free and additive-free, is convenient, is economic, and works under mild conditions, and the as-synthesized ZnO is uniform, single crystalline, of high purity, and morphology controllable. The solid ZnO twinning obtained in the solution is also important in many potential applications. Control experiments and evolution exploration shed light on the understanding of nucleation and growth of nanomaterials at the air−water interface as well as the ZnO twinning evolution. Moreover, the troughlike ZnO, due to its particular morphology and novel optical property, may find vast applications in nanodevice construction and UV−blue light emission devices.

Acknowledgment. The authors gratefully acknowledge the financial support from the National Natural Science Foundation of China (No. 20475052) and the National Key Basic Research Development project research on Human Major Disease Proteomics (No. 2001CB5102).

References and Notes

(1) Huang, M. H.; Mao, S.; Feick, H.; Yan, H.; Wu, Y.; Kind, H.; Weber, K.; Russo, R.; Yang, P. *Science*, **2001**, *292*, 1897.
(2) Govender, K.; Boyle, D. S.; Ö Brien, P.; Binks, D.; West, D.; Coleman. D. *Adv. Mater.* **2002**, *14*, 17.
(3) Choy, J. H.; Jang, E. S.; Won, J. H.; Chuang, J. H.; Jang, D. J.; Kim, Y. W. *Adv. Mater.* **2003**, *15*, 1911.
(4) Liu, C. H.; Zapien, J. A.; Yao, Y.; Meng, X. M.; Lee, C. S.; Fan, S. S.; Lifshitz, Y.; Lee, S. T. *Adv.* Mater. **2003**, *15*, 838.
(5) Yang, J. L.; An, S. J.; Park, W. I.; Yi, G. C.; Choi, W. Y. *Adv. Mater.* **2004**, *16*, 1661
(6) Wan, Q.; Li, Q. H.; Chen, Y. J.; Wang, T. H.; He, X. L.; Gao, X. G.; Li, J. P. *Appl. Phys. Lett.* **2004,** *84*, 16.
(7) Harnack, O.; Pacholski, C.; Weller, H.; Yasuda, A.; Wessel, J. M. *Nano. Lett.* **2003**, *3*, 1097.
(8) Zhu, Y. W.; Zhang, H. Z.; Sun, X. C.; Feng, S. Q.; Xu, J.; Zhao, Q.; Xiang, B.; Wang, R. M.; Yua, D. P. *Appl. Phys. Lett.* **2003**, *83*, 7.
(9) Minami, T., Ida, S.; Miyata, T.; Minamino, Y. *Thin Solid Films*. **2003**, *445*, 268.
(10) Katoh, R.; Furube, A.; Hara, K.; Murata, S.; Sugihara, H.; Arakawa, H.; Tachiya, M. *J. Phys. Chem. B* **2002**, *106*, 12957.
(11) Sharma, P.; Kumar, S.; Sreenivas, K. *J. Mater. Res.* **2003**, *18*, 545.
(12) Yin, M.; Gu, Y.; Kuskovsky, I. L.; Andelman, T.; Zhu, Y. M.; Neumark, G. F.; O'Brien, S. *J. Am.* Chem. *Soc*. **2004**, *126*, 6206.
(13) Lyu, S. C.; Zhang, Y.; Lee, C. J.; Ruh, H.; Lee, H. J. *Chem. Mater*. **2003**, *15*, 3294.
(14) Chang, P. C.; Fan, Z. Y.; Wang, D. W.; Tseng, W. Y.; Chiou, W. A.; Hong, J.; Lu, J. G. *Chem. Mater*. **2004**, *16*, 5133.
(15) Lao, J. Y.; Huang, J. Y.; Wang, D. Z.; Ren, Z. F. *Nano Lett*. **2003**, *3*, 235.
(16) Kong, X. Y.; Wang, Z. L. *Appl. Phys. Lett*. **2004**, *84*, 975.
(17) Ledwith, D., Pillai, S. C., Watson, G. W., Kelly, J. M. *Chem. Commun*. **2004**, 2294.
(18) Zhang, H.; Yang, D. R.; Ji, Y. J.; Ma, X. Y.; Xu, J.; Que, D. L. *J. Phys. Chem. B* **2004**, *108*, 3955.
(19) Gao, X. D.; Li, X. M.; Yu, W. D. *J. Phys. Chem. B* **2004**, *109*, 1155.
(20) Li, F.; Ding, D.; Gao, P. X.; Xin, X. Q.; Wang, Z. L. *Angew. Chem., Int. Ed.* **2004**, *43*, 5238.
(21) Liu, B.; Zeng, H. C. *J. Am. Chem. Soc*. **2004**, *126*, 16744.
(22) Jiang, C. L.; Zhang, W. Q.; Zou, G. F.; Yu, W. C.; Qian, Y. T. *J. Phys. Chem. B* **2005**, *109*, 1361.
(23) Vayssieres L.; Keis, K.; Lindquest, S. E.; Hagfeldt A. *J. Phys. Chem. B* **2001**, *105*, 3350.
(24) Vayssieres L.; Keis, K.; Lindquest, S. E.; Hagfeldt A. *Chem. Mater*. **2001**, *13*, 12.
(25) Boyle, D. S.; Govender, K.; O'Brien, P. *Chem. Commun*. **2002**, 80.
(26) Govender, K.; Boyle, D. S.; Kenway, P. B.; O'Brien, P. *J. Mater. Chem*. **2004**, *14*, 2575.
(27) Wang, B. G.; Shi, E. W.; Zhong, W. Z. *Cryst. Res. Technol*. **1998**, *33*, 937.
(28) Vanheusden, K.; Seager, C. H.; Warren, W. L.; Tallant, D. R.; Voigt, J. A. *Appl. Phys. Lett*. **1996**, *68*, 403.
(29) Wu, X. L.; Siu, G. G.; Fu, C. L.; Ong, H. C. *Appl. Phys. Lett*. **2001**, *78*, 2285.
(30) Wu, J, J.; Liu, S. C. *Adv. Mater.* **2002**, *14*, 215.